Available online at www.sciencedirect.com
SCIENCE DIRECT
Catalysis Today 107–108 (2005) 671–675
CATALYSIS TODAY
www.elsevier.com/locate/cattod

Effect of low steam/carbon ratio on water gas shift reaction

Renan Tavares Figueiredo [a,*], André Luis Dantas Ramos [a], Heloysa Martins Carvalho de Andrade [b], J.L.G. Fierro [c]

[a] *Laboratório de Catálise, Instituto de Tecnologia e Pesquisa, Universidade Tiradentes, Avenida Murilo Dantas, 300, Bairro Farolândia, CEP 49032-490 Aracaju, SE, Brazil*
[b] *Instituto de Química Universidade Federal da Bahia (UFBA), Campus Universitário de Ondina, CE 40170-290 Salvador, Bahia, Brazil*
[c] *Instituto de Catalisis y Petroleoquímica, ICP/CSIC, Campus Universidad Autonoma de Madrid, 28049 Madrid, Spain*

Available online 18 August 2005

Abstract

$Cu/ZnO/Al_2O_3$ catalysts prepared by reverse co-precipitation and an industrial catalyst were used for the low-temperature water gas shift reaction. The catalysts were characterized by chemical analysis (atomic absorption spectroscopy), BET surface area, nitrous oxide chemisorption, X-ray diffraction (XRD), temperature-programmed reduction (TPR), X-ray photoelectron spectroscopy (XPS) and catalytic activity in the target reaction. The catalyst prepared by reverse co-precipitation showed higher BET and copper surface areas, as well as higher catalytic activity. XRD patterns showed that the aurichalcite and hydrozincite precursors were converted into crystalline CuO and ZnO oxides when calcined in air at 623 K. TPR profiles revealed that Cu(I) oxide forms prior to Cu. Binding energies corresponding to several copper states on fresh catalysts were observed by XPS, but copper was in the metallic state during the reaction conditions (reduced catalyst). By varying the catalytic reaction conditions, such as vapor/carbon ratio and the time of contact, it is possible to obtain different conversion rates of carbon monoxide and thus operate under conditions of lower vapor consumption.

Keywords: Low-temperature water gas shift reaction; Cu/Zn/Al catalysts; Copper dispersion; Reduction

1. Introduction

The current world energy situation imposes certain economic measures. Energy saving is a widespread target in industry and is the focus of growing interest. For ammonia production, this can be achieved by varying the vapor/carbon ratio in the synthesis gas production step [1]. However, some obstacles need to be overcome, especially in specific industrial units such as the primary reformer and CO converter at low and high temperatures [2]. These obstacles include: (i) a high risk of coke deposition and increase in CH_4 concentration at the reformer outflow; (ii) the formation of (oxygenated) by-products in the CO converter at high temperature; (iii) the possibility of poison reversibility in the CO converter at low temperature; (iv) higher CO concentrations in the CO converter outflow at low and high temperatures.

The conversion of carbon monoxide and steam to produce carbon dioxide and hydrogen is known as the water gas shift reaction (WGSR) and is used industrially to increase hydrogen concentrations and to eliminate carbon monoxide from the flow of synthesis gas in the production of ammonia. The chemistry and catalysis of this reaction have been studied intensively [3,4] and the development of $Cu/ZnO/Al_2O_3$ catalysts has been applied in the industrial production of ammonia due to economic interest in increasing the production of hydrogen. In addition, carbon monoxide should be completely removed to protect the catalysts used for ammonia synthesis.

A $Cu/ZnO/Al_2O_3$ catalyst is used industrially in the WGSR reaction and, with some modifications, for methanol synthesis. As the synthesis gas contains $H_2/CO/CO_2$, the following reactions may occur during the catalytic process:

$$H_2O + CO \leftrightarrow CO_2 + H_2 \quad (1)$$

$$CO + 2H_2 \leftrightarrow CH_3OH \quad (2)$$

$$CO_2 + 3H_2 \leftrightarrow CH_3OH + H_2O \quad (3)$$

* Corresponding author. Tel.: +55 79 218 2115.
E-mail address: renantf@infonet.com.br (R.T. Figueiredo).

0920-5861/$ – see front matter © 2005 Elsevier B.V. All rights reserved.
doi:10.1016/j.cattod.2005.07.050

Since the reaction of displacement of the water gas can be represented by reaction (1) and methanol synthesis by reactions (2) and (3), understanding of the adsorption mechanism of the reactants on the active sites of the catalyst is required to select the course of the reaction [5]. According to Campbell and Daube [6], the dissociation of water is the rate-determining step and a vapor excess will define the course of the reaction by blocking the active sites, preventing the adsorption of hydrogen and its reaction with formate ions to produce methanol.

In this work, the effect of the steam/carbon ratio on CO conversion in a low-temperature converter was studied. It was considered that the drawbacks in subsequent units mentioned previously would also be improved by varying the steam/carbon ratio, and therefore we used normal industrial conditions. Results are presented showing the effects of the steam/carbon ratio and time of contact on the catalytic activity.

2. Experimental

2.1. Catalyst preparation

The catalysts CZA were prepared by the co-precipitation of Cu^{2+} and Zn^{2+} cations, and then mixing with $Al(OH)_3$ precipitated separately from nitrate solutions (0.5 M), using a Na_2CO_3 solution (0.3 M), at 343 K. The suspension was stirred for 1 h and cooled under stirring for a further 1 h. The final pH was 7.8–8.0. After washing with de-ionized water at 343 K, up to 0.2 ppm [Na^+], the solid was dried at 383 K for 12 h and calcined at 623 K for 4 h. A catalyst, labeled CZA, with the nominal composition of Cu/Zn/Al = 40:45:15, was prepared using the reverse co-precipitation method, where Cu^{2+} and Zn^{2+} were co-precipitated simultaneously and later on mixed with the Al^{3+} phase precipitated separately. The precipitation conditions are described elsewhere [7]. The precipitate was dried at 383 K overnight and calcined in air at 623 K for 4 h. An industrial catalyst, named IND, was used as reference.

2.2. Catalyst characterization

Chemical analyses of Cu, Zn and Al by atomic absorption were carried out on dried samples using a Perkin-Elmer 3030 spectrophotometer. The BET surface area of the catalyst was calculated from the nitrogen adsorption isotherm at 77 K measured in a Micromeritics 2100 apparatus. Chemisorption of nitrous oxide was measured in a Micromeritics 300 apparatus equipped with a thermal conductivity detector. Typically, 0.3 g of the catalyst was reduced in a 10% H_2/He mixture at a flow rate of 50 ml/min. The catalyst sample was heated at 4 K/min to 493 K for 1 h and then subjected to degassing at 353 K for 1 h. Pulses of nitrous oxide diluted in an N_2 flow were allowed to flow through the catalyst at 353 K until no N_2O adsorption was detected. The amount of N_2O chemisorbed in each pulse could be calculated from the difference between the pulse area when the surface was saturated and the area obtained for each pulse. For calculation, it was assumed that the Cu/N_2O ratio was 2 and that the copper crystallography planes (1 0 0), (1 1 1) and (1 1 0) were equally present in the sample, which produced a mean atomic surface area for copper of 7.41 $Å^2$ [8,9].

Powder X-ray diffraction (XRD) patterns of CZA catalyst were recorded on a Seifert diffractometer using nickel-filtered Cu Kα radiation (λ = 0.1542 nm). XRD patterns were recorded for the precursors and for samples after calcination at 623 K under an air flow. Temperature-programmed reduction (TPR) experiments were carried out in an automatic Micromeritics 3000 apparatus interfaced to a data workstation. Since water is produced during reduction, the gas exiting from the reactor was passed through a cold trap before entering the thermal conductivity detector. Calcined samples (30 mg) were heated at 4 K/min from 290 to 750 K in a 10% H_2/N_2 mixture at 80 ml/min. Photoelectron spectra were acquired with a VG Escalb 200R spectrometer equipped with a hemispherical electron analyzer and a Mg Kα 120 W X-ray source interfaced to a data station. Powder samples were pressed into small aluminum cylinders and then mounted on a sample rod, placed in a pretreatment chamber and heated under vacuum at 373 K for 1 h prior to being moved to the analysis chamber. After analysis, the same catalyst sample was moved to the pretreatment chamber and reduced in situ by hydrogen at 493 K. The pressure in the ion-pumped analysis chamber was below 3×10^{-9} Torr (1 Torr = 133.33 N/m^2) during data acquisition. Spectra were collected from 20 to 90 min, depending on peak intensity, at a pass energy of 20 eV (1 eV = 1.602×10^{-19} J), which is typical for high-resolution conditions. The intensities were estimated by calculating the integral of each peak after smoothing and subtracting the S-shaped background and fitting the experimental curve to a mixture of Lorentzian and Gaussian lines of variable proportions. All binding energies (BE) were referenced to the C 1s line at 284.9 eV. This reference gave BE values within an accuracy of ±0.2 eV.

2.3. Catalytic tests

Activity measurements were carried out using a fixed-bed tubular reactor consisting of a 40 cm stainless steel tube (i.d. 1.3 cm) operated at atmospheric pressure. A washing flask containing sulfuric acid was used to remove water from the exit gases. The feed gas, with volumetric composition of 0.25% CH_4, 16.5% CO_2, 3.2% CO, 0.2% Ar, 20.5% N_2 and 59.3% H_2, was supplied by an industrial ammonia plant. Steam was supplied to the reactor from a saturator containing distilled water under rigorous temperature control to allow accurate variation of the vapor/gas (V/G) molar ratio. The space velocity was 4500 h^{-1} during the reaction tests. Reaction conditions to avoid mass transfer

limitations were established for activity testing. The feed gas and reaction effluents were analyzed using a TRACE GC ThermoQuest chromatograph equipped with Porapak Q and Molecular Seive 13X columns, with a thermal conductivity detector, a flame ionization detector and a methanator with a 5 Å molecular sieve column and a Porapak Q column. Powdered catalyst samples (0.05–0.10 g, −100/+150 mesh) were activated in situ by heating to 393 K in N_2 flow and then to 493 K in a 10% H_2/N_2 mixture at 4 K/min. Before testing, the catalyst was reduced for a further 2 h at 493 K and space velocity of 4500 h^{-1}.

3. Results and discussion

3.1. Preparation and characterization

Results for the chemical composition, BET area and copper surface areas of calcined catalysts are compiled in Table 1. Metal contents in the CZA catalysts were close to the nominal values. Chemical analysis of the IND catalyst was reported by the manufacturer. Both the BET area and copper surface areas of the CZA catalyst were greater than for the commercial catalyst, which can explain the higher dispersion of this catalyst.

Fig. 1A shows an XRD pattern for fresh (dried) CZA catalyst. The aurichalcite crystalline phase $(CuZn)_5(CO_3)_2(OH)_6$ (JCPDS 17–743) and hydrozincite $Zn_5(CO_3)_2(OH)_6$ (JCPDS 10–1458) are probably present as well, but unambiguous assignment of their reflections cannot be made due to their large width and the vicinity of more intense reflection peaks due to zinchian–malachite and aurichalcite, respectively. However, the phases detected correlate well with previous results for systems with similar Cu/Zn/Al composition [10–13].

Calcination of CZA catalysts under an air flow yielded metallic oxides after carbon dioxide and water elimination, as can be observed from Fig. 1B. Intense reflections of CuO and ZnO phases can be observed, indicating good crystallinity of these phases. Low Al_2O_3 peak intensities indicate the presence of a poorly crystallized γ-Al_2O_3 phase. The formation of $CuAl_2O_4$ spinel can be ruled out because it is generally formed when low calcination temperatures are used, with Cu^{2+} ions in a distorted octahedron. Other phases containing any of the metals used in the system are most likely to be present. However, due to their poor and highly disordered crystallization or to their small crystal size, they cannot be detected by XRD.

Table 1
Chemical composition and physical–chemical properties of fresh catalysts

Catalysts	CZA	IND
Composition, Cu/Zn/Al (wt.%)	39:44:17	42:47:10[a]
S_{BET} (m^2/g)	100.4	53.4
S_{Cu} (m^2/g)	61.3	39.3
Dispersion (%)	13.8	8.9

[a] Carbon (graphite), sulfur, chlorine and other heavy metals represent 1% of the catalyst.

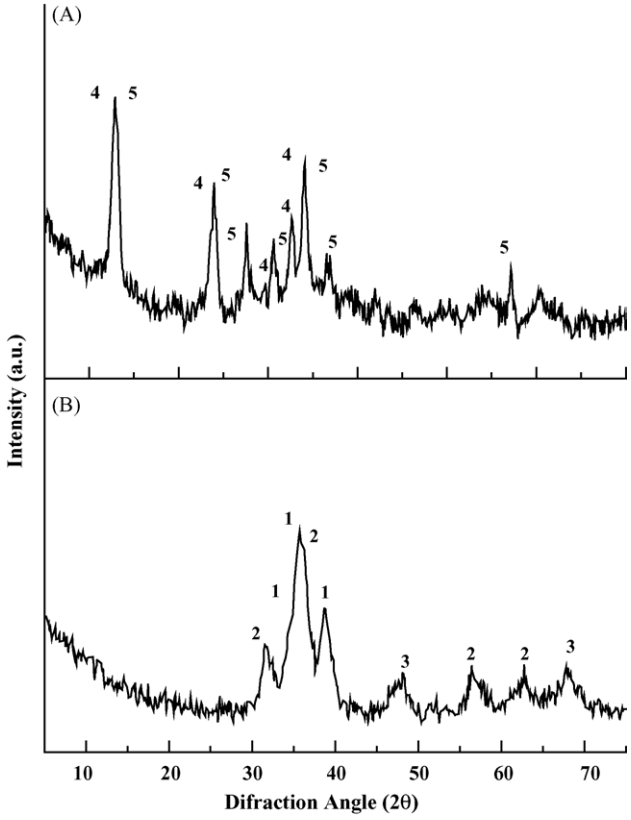

Fig. 1. X-ray diffraction patterns of a CZA catalyst during different stages of treatment: (A) fresh (dried) sample and (B) calcined catalyst. Diffraction lines of: (1) CuO; (2) ZnO; (3) (γ-Al_2O_3); (4) auricalcite—$(ZnCu)_5(CO_3)_2(OH)_6$; (5) $(Cu_xZn_{1-x})_5(CO_3)_2(OH)_6$, $x = 0.1$, 0.2 and 0.3.

Fig. 2 shows the TPR profile of the CZA catalyst between 373 and 573 K. Properties such as Cu^{2+} dispersion and its chemical environment, the crystal size of CuO and the degree of crystallization, among others, are key properties in

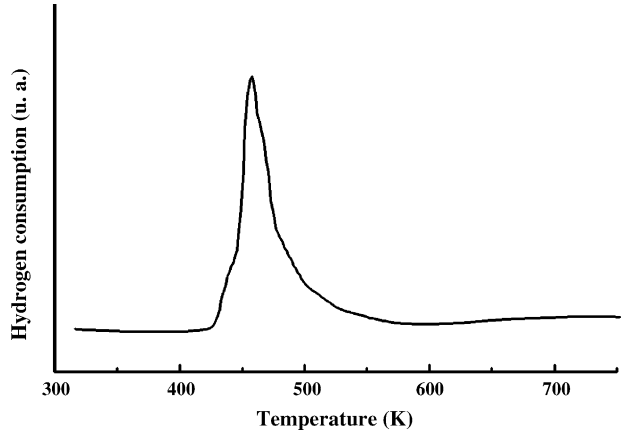

Fig. 2. Temperature-programmed reduction (TPR) profiles of calcined samples (measured as H_2 consumption in a thermal conductivity detector): CZA.

determining reduction behavior. Therefore, TPR is a very valuable tool to detect alterations in the Cu^{2+} state. Estimation of the extent of reduction from the integral of these curves revealed that copper oxide was stoichiometrically reduced to Cu^0. The broadened TPR profile indicates superposition of two or three peaks. These could represent indefinite structures of copper oxide in these catalysts. Previous works have demonstrated that, as temperature increases, at least four forms of Cu^{2+} in calcined catalysts are reduced: copper in the ZnO lattice, in amorphous Cu oxide phases, in crystalline CuO and Cu^{2+} in the Al_2O_3 phase [9–14]. Our profiles show a shoulder at 430–445 K, which can be assigned to reduction of Cu^{2+} to Cu^{1+} [3–18], a peak at 455 K, which can be assigned to the reduction of Cu^{2+} and/or Cu^{1+} to Cu^0 species [3,19], and a shoulder at 480 K, which can be assigned to copper species interacting with the Al^{2+} phase, which is more difficult to reduce [14–19]. The precursor TPR plot showed a different profile and peak positions.

The metallic particle size distribution in the catalysts and the reduction behavior of calcined samples were a consequence of the interaction between Cu^{2+}, Zn^{2+} and Al^{2+} phases, the dispersion of Cu^{2+} phases in the ZnO–Al_2O_3 matrix and the CuO crystal size.

The chemical state and composition of the fresh and reduced catalysts were determined by X-ray photoelectron spectroscopy (XPS). The results are presented in Table 2. Numbers in parentheses correspond to the percentage peak area in relation to the total area for that element. Significant differences were observed for the Cu $2p_{3/2}$ binding energy. The essential characteristics of the Cu 2p spectrum were always observed in non-reduced samples (vacuum or re-oxidized). The BE of the Cu $2p_{3/2}$ peak at approximately 933 eV and the presence of satellite lines are indicative of the presence of a CuO phase [3,20]. The component at 935 eV can be assigned to Cu^{2+} ions interacting with the Al_2O_3 phase, i.e. a $CuAl_2O_4$ spinel-like structure [21]. After reduction in H_2, copper species were reduced to metallic copper, as confirmed by the low BE at 932.4 eV and by the absence of satellite lines. Metallic copper should be the preferred state under the reaction conditions used. The atomic Cu/Zn ratio increased when the sample was reduced

Table 2
Binding energy (eV) of internal electrons and superficial atomic ratios

Catalyst	Cu $2p_{3/2}$	Cu/Zn	Al/Zn
CZA (vacuum)	932.9 (87) 934.0 (13)	0.611	0.229
CZA[a] (T = 220 °C)	932.4 932.8 (86)	0.449	0.237
CZA_r[b] (re-oxidized)	935.2 (14)	0.509	0.201
CZA[a] (T = 220 °C)	932.4	0.239	0.216
IND (vacuum)	933.1	1.562	3.837

[a] Reduced at 220 °C.
[b] Re-oxidized.

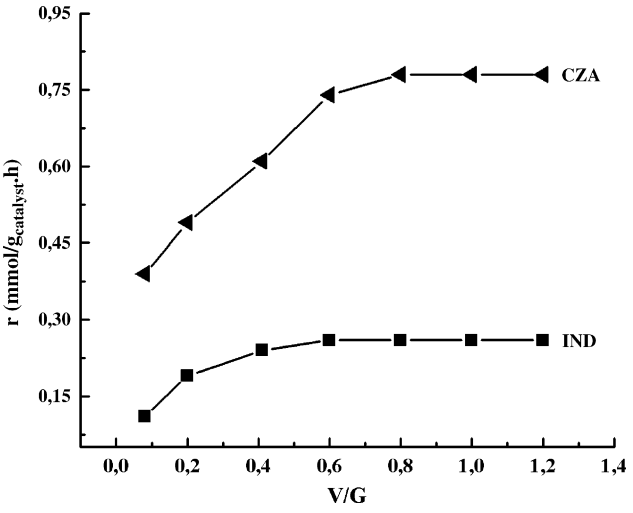

Fig. 3. CO reaction rate expressed as r (mmol/$g_{catalyst}$ h) as a function of the steam/carbon ratio.

and also when it was re-oxidized, suggesting re-dispersion of the Cu metallic phase. The Al/Zn ratio did not show such behavior. These results are in agreement with those previously reported [7]. For the IND catalyst, the Cu $2p_{3/2}$ binding energy suggests that only CuO is present on the fresh catalyst. The significantly higher Cu/Zn and Al/Zn ratios compared to the CZA catalyst should be highlighted, indicating enrichment in Al and Cu on the surface of IND catalyst.

Fig. 3 presents the activity in the water gas shift reaction expressed as millimoles CO converted per hour and per kilogram of catalyst (CZA and IND) as a function of the steam/carbon ratio. All the catalysts were completely selective for the low-temperature shift reaction. The CZA catalyst showed higher activity than the IND reference catalyst. This result is in agreement with previous works, which claimed that the behavior of Cu/ZnO/Al_2O_3 catalysts

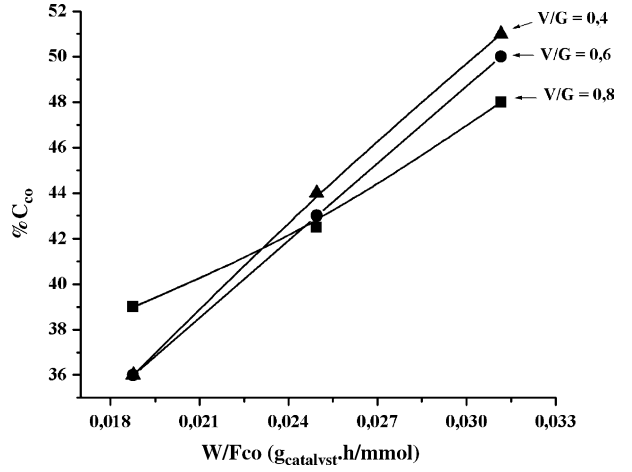

Fig. 4. Conversion of CO expressed as percentage (%C_{CO}) as a function of (W/F_{CO}) ratio for CZA catalyst, at different vapor/carbon ratio (V/G).

depends only on the availability of a Cu surface and that the WGSR at low temperature is not sensitive to structure [2,4]. Since the CZA catalyst showed higher copper surface area and dispersion, the copper particles must be smaller. Therefore, it is reasonable to expect that the activity of this catalyst for CO conversion would be higher than that of IND catalyst. It should also be emphasized that both catalysts displayed the same conversion profiles over the whole V/G range of the experiment. Above V/G = 0.7–0.8, CO conversion remains practically constant, which agrees with the higher copper surface area and dispersion found for the CZA catalyst.

Fig. 4 shows the CO conversion variation as a function of the time of contact (W/F_{CO}) for the CZA catalyst. Three different regions can be distinguished. Region I ($W/F_{CO} < 0.024$) is characterized by higher CO conversion at higher V/G ratios. In the second region, $\pm 0.024 < W/F_{CO} < \pm 0.027$, small variations in CO conversion with the steam/carbon ratio are observed. Finally, in Region III ($W/F_{CO} > 0.027$) higher CO conversion was obtained at lower V/G ratios. It can be speculated that differences in surface properties may explain the different behavior of the CZA catalyst under different conditions.

4. Conclusions

The catalysts used in this work (homemade and industrial) showed the same CO conversion profiles in the low-temperature shift reaction. The conversion of CO increased continuously with increasing steam/carbon ratio, until reaching a constant value. The CZA catalyst showed higher conversion than the commercial catalyst. The time of contact (W/F_{CO}) and steam/carbon ratio (V/G) can be used as basic tools to reduce the amount of vapor introduced to the reaction system. The influence of the time of contact on the conversion showed three different regions, with higher conversion for a lower V/G ratio at lower contact time, and the opposite at a higher time of contact.

Acknowledgments

The authors acknowledge the financial support of UNIT, BNB, FAP-SE, CENPES-PETROBRAS and FAFEN-PETROBRÁS.

References

[1] B.J. Hansen, J.H. Carstensen, P.S. Pedersen, AICHE Ammonia Safety Symposium, Denver, 1988, p. 77.
[2] B.J. Hansen, J.H. Carstensen, A.G. Romero, PEQUIVEN, Venezuela, 1981, p. 1.
[3] Y. Okamoto, Y. Konishi, K. Fukino, T. Inamaka, S. Teranish, International Congress on Catalysis, vol. V, Berlin, 1984, p. 159.
[4] M.G. Kalchev, A.A. Andreev, N.S. Zotov, Kinet. Catal. 36 (6) (1995) 821.
[5] G. Ghiotti, F. Boccuzzi, Catal. Rev. Sci. Eng. 29 (2–3) (1987) 151.
[6] C.T. Campbell, K.A. Daube, J. Catal. 104 (1987) 109.
[7] R.T. Figueiredo, M. Lopez-Granados, A. Martinez-Arias, J.L.G. Fierro, J. Catal. 178 (1) (1998) 146.
[8] J.J.F. Scholten, Stud. Surf. Sci. Catal. 3 (1979) 685.
[9] J.W. Evans, M.S. Wainwright, A.J. Bridgewater, D.J. Young, Appl. Catal. 7 (1983) 75.
[10] P. Porta, M. Campa, G. Fierro, M. Lo Jacono, G. Moretti, L. Stoppa, J. Mater. Chem. 3 (1993) 505.
[11] R.G. Herman, K. Klier, G.W. Simmons, P.B. Finn, J.B. Bulko, T.P. Kobylinski, J. Catal. 56 (1979) 407.
[12] G. Sengupta, R.K. Sharma, V.B. Sharma, K.K. Misha, M.L. Kundu, R.M. Sanyal, S. Dutta, J. Solid State Chem. 115 (1995) 204.
[13] S. Fujita, A.A.M. Satriyo, G.C. Shen, N. Takezawa, Catal. Lett. 34 (1995) 85.
[14] T.A. Osinga, B.G. Linsen, W.P. van Beek, J. Catal. 7 (1967) 277.
[15] G. Fierro, M. Lo Jacomo, M. Inversi, P. Porta, R. Lavecchia, F. Cioci, J. Catal. 148 (1994) 709.
[16] Yu.B. Naumov, L. Pavlov, A.A. Vasilevich, A.M. Laekseev, É.A. Novikov, G.G. Schibrya, Kinet. Catal. 27 (4) (1986) 818.
[17] G.G. Schibrya, A.M. Alekseev, B.G. Lyudkovskaya, E.N. Kalistratova, I. Gille, G.S. Shitikova, A.Ya. Volyntina, A.S. Teleshova, E.P. Kovtunenko, Kinet. Catal. 21 (1) (1980) 231.
[18] W.D. Bond, J. Phys. Chem. 66 (1962) 1573.
[19] M.G. Kalchev, A.A. Andreev, N.S. Zotov, Kinet. Catal. 36 (6) (1995) 821.
[20] G. Moretti, S.D. Rossi, G. Ferraris, Appl. Surf. Sci. 45 (1990) 341.
[21] A. Sepúlveda, C. Marquez, I. Rodriguez-Ramos, A. Guerrero-Ruiz, J.L.G. Fierro, Surf. Interface Anal. 20 (1993) 1067.